

High- K isomers in a self-consistent mean-field approach with the Gogny force

L. M. Robledo^{1,2,*}

¹*Departamento de Física Teórica and CIAFF, Universidad Autónoma de Madrid, E-28049 Madrid, Spain*

²*Center for Computational Simulation, Universidad Politécnica de Madrid, Campus de Montegancedo, Bohadilla del Monte, E-28660-Madrid, Spain*

(Dated: December 6, 2023)

High- K isomeric states in even-even and odd-mass nuclei are described within a mean-field framework with full blocking and using the finite range Gogny force. Theoretical calculations of low energy spectra of several nuclei across the nuclear chart are compared with equal filling approximation results and experimental data. Despite the global character of the employed interactions, a good agreement between the different many-body methods and experimental data is found.

I. INTRODUCTION

The spectrum of atomic nuclei presents a rich variety of situations, ranging from collective states, where many nucleons participate coherently to the dynamic, to single particle excitations, where particles jump from occupied orbits to unoccupied ones. The former are easier to identify as many of their characteristics are very robust as they are dictated by symmetries or the lack of them, and they traditionally lie down at low excitations energies. On the other hand, single particle excitations (one-particle one-hole excitations, two-particle two-hole, etc.) are far more numerous, but lie higher up in excitation energy and their electromagnetic decay is far weaker than in the collective case. Among the large variety of single particle excitations, high- K isomers occupy a prominent place due to their large projection of angular momentum along the z axis (the so-called K quantum number) [1–7]. High- K isomers require rather uncommon combinations of large Ω single-particle states close to the Fermi level¹, and therefore they are only present in specific regions of the nuclear chart. In addition, their large K -value represent a strong hindrance in the electromagnetic transition strengths to the surrounding low- K states, resulting in long lifetimes that facilitate their experimental characterization while providing an excellent target for theoretical studies. High- K isomer physics can be of great importance in different scenarios like energy storage, therapeutic uses or the understanding of stellar nucleosynthesis [8, 9], just to mention a few. In the later case, the high temperature environment makes possible to populate high- K isomeric states that act, thereby, as potential waiting points in the r-process mechanisms - the so-called astromers [10]. For instance, recent studies suggested that long-lived isomers could impact the kilonova light curve produced by the nucleosynthesis of heavy elements in neutron star mergers [10–12], calling for theoretical calculations of long-lived isomers in the neutron-rich

region of the nuclear chart.

Mic-mac models based on a combination of a microscopic Woods-Saxon potential and a macroscopic deformation dependent liquid drop energy. Due to its simplicity, they are very popular in the description of many nuclear structure phenomena including high- K isomers [13, 14]. Initial calculations of high- K states were initially restricted to fixed deformation parameters (often assumed axially symmetric). The situation changed with the development of the multi-qp potential energy surface method [15] (see Ref [14] for a thorough application of the method in the super-heavy region). It allows a more flexible characterization of the deformation of isomeric states including triaxial effects. This flexibility is akin to the expected consequences of self-consistent blocking. In mic-mac models, pairing is often considered through a monopole pairing force treated at the Bardeen-Cooper-Schrieffer (BCS) level. In some calculations, the Lipkin-Nogami (LN) method is used to include dynamic correlations beyond mean field. The main difficulty of mic-mac models is the difficulty to obtain wave functions beyond those Wood-Saxon + BCS mean field ones. This represents a strong limitation in the calculation of the decay out of high- K states. Also, the success of the method in describing experimental data relies on a carefully refitting of the parameters to specific and limited regions of the nuclear chart restricting its predicting power.

The projected shell model (PSM) [16] is a semi-microscopic theoretical tool often used to study high- K isomers [17]. It uses a combination of intrinsic multi-quasiparticle excitations projected to good angular momentum to obtain sophisticated and highly correlated many body wave functions. Undoubtedly, this aspect represents an advantage in the description of the decay out of high- K isomeric states. The multi-quasiparticle configurations are built on top of a common vacuum with fixed deformation and pairing gap and therefore they can only incorporate the effect of self-consistent blocking through the subsequent linear combination of excitations limiting the possibilities of rearrangement of deformation and pairing correlations of multi-quasiparticle excitations. This represents an important drawback of the method. The configuration space spans two major oscillator shells both for protons and neutron (not necessarily

* luis.robledo@uam.es

¹ In the following, both K and Ω represent the projection of angular momentum along z axis. K is for quasiparticle excitations while Ω is for single particle orbitals.

the same in both cases) and the pairing plus quadrupole (P+Q) Hamiltonian [18] is used for the interaction. The model has proved to be very successful in describing high spin physics in various regions of the nuclear chart. Although the Hamiltonian is expected to embrace the two most relevant aspects of the nuclear residual interaction (quadrupole and pairing collectivities), it is constrained to deal with a fixed deformation parameter, limiting its applicability to situations where the different excitations of the system have similar deformations and pairing properties. This limitation prevents a more general characterization of the decay out of high- K states. Also, the parameters of the Hamiltonian are obtained from experimental data limiting its applicability in new regions of the nuclear chart. Recently [19] the PSM has been extended to handle up to ten-quasiparticle excitations by using the pfaffian formula of [20, 21].

Previous results concerning two-quasiparticles excitations in actinide and super-heavy nuclei obtained with Gogny D1S have already been discussed in [22]. Time reversal symmetry was preserved in most of the applications and only in a few examples it was allowed to break. In addition, four and higher number of quasiparticle excitations were not taken into account. Other topics discussed in the present paper (see below) were not considered in that reference.

The purpose of this paper is to show how high- K isomeric states can be successfully described at the mean-field level with the blocking method and density dependent finite range forces. Two and four-quasiparticles excitations are considered to illustrate the method, but the formalism can be applied to an arbitrary number of quasiparticles excitations. The mechanism responsible for the reduction of the excitation energy of the multiquasiparticle configurations as compared to the perturbative estimation is identified as the quenching of pairing correlations. The results obtained with the blocking formalism are compared with the equal filling approximation neglecting the time-odd terms of the functional. The excellent agreement between both methods suggests a minor role of time odd-field in the description of excitation energies. The nuclei chosen to illustrate the method are all even-even nuclei and belong to the category of being well characterized experimentally. Most interesting applications considering astromers [10, 12] will be deferred to future publications. As discussed below, the main advantages of the present proposal versus other approaches discussed above are the use of self-consistent blocking that allows for different deformation parameters and pairing properties for different excitations. Also, the universal character of the Gogny force and the good reproduction of experimental data in the considered nuclei give us confidence on the predictive power of the proposal. Last but not least, the wave functions obtained can be used in sophisticated calculations of the decay mechanism including symmetry restoration. The universal character of the Gogny force also allows for a consistent and same-quality description of the decay products (members of rotational

band, triaxial configuration, other multi-quasiparticle excitations, etc) facilitating the interpretation of the decay out mechanism of high- K isomers.

The paper is structured as follows. In Sec. II we present the theoretical methods employed for the calculation of multi-quasiparticles excitations. In Sec. III we present the results for high- K isomers and low energy spectra for several nuclei across the nuclear chart. Finally, in Sec. IV we summarize the main results and outlook future work.

II. THEORETICAL METHODS

The self-consistent description of high- K isomers is based on the Hartree-Fock-Bogoliubov (HFB) approximation with blocking [18, 23]. In the HFB method, the concept of quasiparticle is introduced by defining quasiparticle creation and annihilation operators

$$\begin{pmatrix} \beta \\ \beta^\dagger \end{pmatrix} = \begin{pmatrix} U^+ & V^+ \\ V^T & U^T \end{pmatrix} \begin{pmatrix} c \\ c^\dagger \end{pmatrix} \equiv W^+ \begin{pmatrix} c \\ c^\dagger \end{pmatrix}, \quad (1)$$

as well as the corresponding HFB state $|\Phi\rangle$, vacuum to all the annihilation quasiparticle operators β_μ , i.e. $\beta_\mu|\Phi\rangle = 0$. The label μ indexes the quasiparticle configurations and often contains quantum numbers like parity or projection of angular momentum along the intrinsic z axis (the K quantum number). As the HFB method does not preserve particle number symmetry, an important concept is “number parity” (NP) describing the parity (even or odd) of the number of particles in the different components making $|\Phi\rangle$ and its excitations. Number parity is a symmetry of the system and imposes a superselection rule: wave functions with opposite NP values cannot be mixed together. An even-even nucleus has to be described by a HFB state with even number parity for both protons and neutrons. The quasiparticle operators have odd NP (they involve just creation and annihilation operators) and therefore $\beta_\mu^+|\Phi\rangle$ has opposite NP to that of $|\Phi\rangle$. Genuine excitations of a given system $|\Phi\rangle$ are then given by two-, four-, etc quasiparticles excitations whereas one-, three-, etc quasiparticles excitations correspond to an odd mass system if $|\Phi\rangle$ is an even number of particles wave function.

The Bogoliubov amplitudes U and V are determined by using the variational principle on the HFB energy $E_{HFB} = \langle \Phi | \hat{H} | \Phi \rangle$ leading to the well know HFB equation [18, 23]. The obtained quasiparticle energies E_μ are the ingredients entering the “perturbative” excitation energy $E_{\mu_1} + \dots + E_{\mu_M}$ of a multi-quasiparticle (MQP) excitation $\beta_{\mu_1}^+ \dots \beta_{\mu_M}^+ |\Phi\rangle$. This “perturbative” method is widely used in the literature, see Ref. [22] for an application in super-heavy nuclei with the Gogny force.

As the MQP excitations do not necessarily share the same properties of $|\Phi\rangle$, it is necessary to use a self-consistent procedure where, for each MQP excitation, the U and V amplitudes are determined by using the

variational principle on the MQP energy

$$E_{\mu_1, \dots, \mu_M} = \langle \Phi | \beta_{\mu_M} \dots \beta_{\mu_1} \hat{H} \beta_{\mu_1}^+ \dots \beta_{\mu_M}^+ | \Phi \rangle. \quad (2)$$

When used along with specific constrains on collective parameters this method provides also with potential energy surfaces (PES) for each specific MQP excitation opening up the possibility to study the coupling with collective excitations using the generator coordinate method (GCM) framework.

The best way to handle MQP excitations is by using the ‘‘blocking’’ procedure. In the standard HFB method, the matrix of contractions

$$\mathbb{R} = \begin{pmatrix} \langle \Phi | \beta_{\mu}^{\dagger} \beta_{\nu} | \Phi \rangle & \langle \Phi | \beta_{\mu}^{\dagger} \beta_{\nu}^{\dagger} | \Phi \rangle \\ \langle \Phi | \beta_{\mu} \beta_{\nu} | \Phi \rangle & \langle \Phi | \beta_{\mu} \beta_{\nu}^{\dagger} | \Phi \rangle \end{pmatrix} = \begin{pmatrix} 0 & 0 \\ 0 & \mathbb{I} \end{pmatrix} \quad (3)$$

is connected to the generalized density matrix \mathcal{R} through the W transformation from Eq. (1):

$$\mathcal{R} = \begin{pmatrix} \langle \Phi | c_k^{\dagger} c_l | \Phi \rangle & \langle \Phi | c_k^{\dagger} c_l^{\dagger} | \Phi \rangle \\ \langle \Phi | c_k c_l | \Phi \rangle & \langle \Phi | c_k c_l^{\dagger} | \Phi \rangle \end{pmatrix} = \begin{pmatrix} \rho & \kappa \\ -\kappa^* & 1 - \rho^* \end{pmatrix} = W \mathbb{R} W^{\dagger}. \quad (4)$$

In the MQP case one has to replace $|\Phi\rangle$ by $|\tilde{\Phi}\rangle = \beta_{\mu_1}^+ \dots \beta_{\mu_M}^+ |\Phi\rangle$ which is again a HFB wave function but vacuum of a different set of quasiparticle operators. Therefore, Wick’s theorem is also valid but the contraction matrix is now given by a different expression. In the one-quasiparticle case one has

$$\mathbb{R}_{\mu} = \begin{pmatrix} \mathbb{I}_{\mu} & 0 \\ 0 & \mathbb{I} - \mathbb{I}_{\mu} \end{pmatrix} \quad (5)$$

where the notation

$$(\mathbb{I}_{\mu})_{\sigma\rho} = 1 \quad \text{if } \mu = \sigma = \rho; \quad 0 \text{ otherwise}, \quad (6)$$

has been introduced. The key point of the ‘‘blocking’’ method is the decomposition

$$\mathbb{R}_{\mu} = \mathbb{S}_{\mu} \mathbb{R} \mathbb{S}_{\mu}^{\dagger}, \quad (7)$$

where the ‘‘swap’’ matrix

$$\mathbb{S}_{\mu} = \begin{pmatrix} \mathbb{I} - \mathbb{I}_{\mu} & \mathbb{I}_{\mu} \\ \mathbb{I}_{\mu} & \mathbb{I} - \mathbb{I}_{\mu} \end{pmatrix} \quad (8)$$

has been introduced. When this transformation is applied to the right of a given W Bogoliubov matrix

$$W_{\mu} = W \mathbb{S}_{\mu}, \quad (9)$$

the column μ of U and V^* gets swapped. The ‘‘swap’’ matrix allows to write the density matrix contraction

$$\begin{aligned} \mathcal{R}_{\mu} &= \begin{pmatrix} \langle \tilde{\Phi} | c_k^{\dagger} c_l | \tilde{\Phi} \rangle & \langle \tilde{\Phi} | c_k^{\dagger} c_l^{\dagger} | \tilde{\Phi} \rangle \\ \langle \tilde{\Phi} | c_k c_l | \tilde{\Phi} \rangle & \langle \tilde{\Phi} | c_k c_l^{\dagger} | \tilde{\Phi} \rangle \end{pmatrix} \\ &= W \mathbb{R}_{\mu} W^{\dagger} = W \mathbb{S}_{\mu} \mathbb{R} \mathbb{S}_{\mu}^{\dagger} W^{\dagger} = W_{\mu} \mathbb{R} W_{\mu}^{\dagger}, \end{aligned} \quad (10)$$

that thereby justifies keeping the same formalism as in the ‘‘fully paired’’ case but swapping column μ of the U

and V^* matrices. The generalization to a MQP excitation is straightforward

$$\begin{aligned} \mathbb{R}_{\mu_1, \dots, \mu_M} &= \begin{pmatrix} \sum_{k=1}^M \mathbb{I}_{\mu_k} & 0 \\ 0 & \mathbb{I} - \sum_{k=1}^M \mathbb{I}_{\mu_k} \end{pmatrix} \\ &= \left(\prod_{k=1}^M \mathbb{S}_{\mu_k} \right) \mathbb{R} \left(\prod_{k=M}^1 \mathbb{S}_{\mu_k}^{\dagger} \right), \end{aligned} \quad (11)$$

leading to the definition

$$W_{\mu_1, \dots, \mu_M} = W \left(\prod_{k=1}^M \mathbb{S}_{\mu_k} \right). \quad (12)$$

This expression is equivalent to the swapping of columns μ_1, \dots, μ_M in the U and V^* matrices. Interestingly, this result is in agreement with recent finding [24] showing that the number parity of an HFB state is given by the determinant of the associated W Bogoliubov matrix. Noticing that $\det \mathbb{S}_{\mu_k} = -1$ it is clear that, as expected, the number parity of the multi-quasiparticle excitation is the one of the initial state times $(-1)^M$.

In this work, the calculations are performed using the density dependent finite range Gogny interaction. The density dependence comes in the form of a non-integer power of the spatial density corresponding to the HFB state under consideration and introduces a dependence of the interaction on the state considered. In the present case, the HFB state is a MQP excitation built on a reference HFB wave function $|\Phi\rangle$ and the spatial density to use in the density dependent terms is given by

$$\rho(\vec{R})_{\mu_1, \dots, \mu_M} = \langle \Phi | \beta_{\mu_M} \dots \beta_{\mu_1} \hat{\rho}(\vec{R}) \beta_{\mu_1}^+ \dots \beta_{\mu_M}^+ | \Phi \rangle. \quad (13)$$

This choice is consistent with the fact that the energy of the MQP excitation must be given, at zero order, by the sum of the HFB energy of the reference state $E_0 = \langle \Phi | \hat{H} | \Phi \rangle$ plus the sum of quasiparticle energies $E_{\mu_1} + \dots + E_{\mu_M}$ relative to $|\Phi\rangle$. In order to check this property one possibility is to evaluate $\rho(\vec{R})_{\mu_1, \dots, \mu_M}$ using the quasiparticle representation of the one-body density operator $\hat{\rho}(\vec{R}) = \sum_{i=1}^A \delta(\vec{R} - \vec{r}_i)$ with respect to $|\Phi\rangle$ [18]

$$\hat{\rho}(\vec{R}) = \langle \Phi | \hat{\rho}(\vec{R}) | \Phi \rangle + \sum_{\sigma\sigma'} \rho_{\sigma\sigma'}^{11}(\vec{R}) \beta_{\sigma}^+ \beta_{\sigma'} + \frac{1}{2} (\rho^{20} + \rho^{02}), \quad (14)$$

where the ρ^{20} (ρ^{02}) operator contain two creation (annihilation) quasiparticle operators and therefore its mean value with respect to $|\Phi\rangle$ is zero. Only the first two terms of the above expression contribute to $\rho(\vec{R})_{\mu_1, \dots, \mu_M}$, being the final result

$$\rho(\vec{R})_{\mu_1, \dots, \mu_M} = \rho_0(\vec{R}) + \sum_{\mu=\mu_1}^{\mu_M} \rho_{\mu, \mu}^{11}(\vec{R}). \quad (15)$$

In the expression above, $\rho_0(\vec{R})$ corresponds to the density of the reference state $|\Phi\rangle$

$$\rho_0(\vec{R}) = \langle \Phi | \hat{\rho}(\vec{R}) | \Phi \rangle = \sum_{kl} \varphi_k^*(\vec{R}) \varphi_l(\vec{R}) \rho_{lk}, \quad (16)$$

and $\rho_{\mu,\mu}^{11}$ is the diagonal element of the 11 matrix O^{11} of the one-body operator with matrix elements $f_{ij}(\vec{R})$

$$\rho_{\mu,\mu}^{11}(\vec{R}) = \sum_{ij} f_{ij}(\vec{R})(U_{i\mu}^* U_{j\mu} - V_{j\mu}^* V_{i\mu}), \quad (17)$$

with $f_{ij}(\vec{R}) = \langle i|\delta(\vec{r} - \vec{R})|j\rangle = \varphi_i^*(\vec{R})\varphi_j(\vec{R})$. Assuming that $\rho_0(\vec{R})$ is much larger than $\rho_{\mu,\mu}^{11}(\vec{R})$, one can expand the ρ^α density dependent term as

$$\rho(\vec{R})_{\mu_1,\dots,\mu_M}^\alpha = \rho_0^\alpha(\vec{R}) + \alpha\rho_0^{\alpha-1}(\vec{R}) \sum_{\mu=\mu_1}^{\mu_M} \rho_{\mu,\mu}^{11}(\vec{R}) + \dots \quad (18)$$

In the derivation of the HFB equation for $|\Phi\rangle$ one has to include a ‘‘rearrangement’’ term $\partial\Gamma_{kl}$ in the definition of the Hartree-Fock (HF) Hamiltonian h_{kl} to account for the variation of the density dependent term when $|\Phi\rangle$ is varied [25]. In order to be consistent, the same ‘‘rearrangement’’ term is included in the HF Hamiltonian entering the definition of the matrix $H_{\mu\nu}^{11}$ leading, upon diagonalization, to the definition of the quasiparticle energies E_μ . It turns out that the extra ‘‘rearrangement’’ term to be added to $H_{\mu\mu}^{11}$ is $\alpha\langle\Phi|\rho_0^{\alpha-1}(\vec{R})\rho_{\mu,\mu}^{11}(\vec{R})|\Phi\rangle$, which corresponds to the first order term in the expansion of Eq. (18). See [25] for a detailed derivation in the one-quasiparticle case.

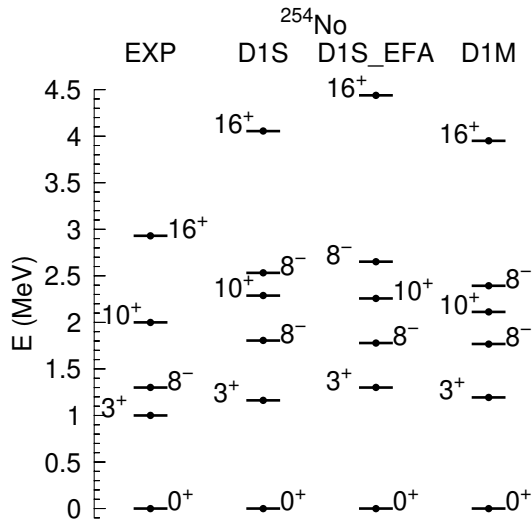


FIG. 1. Comparison of experimental [3, 9, 26, 27] and theoretical results for two- and four-quasiparticles isomeric states in the nucleus ^{254}No . The calculations have been carried out with the D1S and D1M parameterization of the Gogny force and the full blocking procedure and EFA (see text for more details).

A. The Gogny force

As mentioned above, the interaction of choice is the effective density-dependent Gogny force, which is the sum

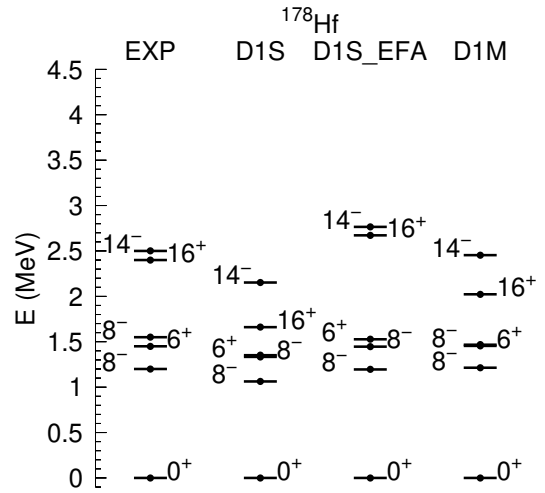


FIG. 2. Comparison of experimental [9] (and references therein) and theoretical results for two- and four-quasiparticles isomeric states in the nucleus ^{178}Hf . The calculations have been carried out with the D1S and D1M parameterization of the Gogny force and the full blocking procedure and EFA (see text for more details).

of a finite-range central potential, a sum of two Gaussians with different ranges, a zero-range two-body spin-orbit potential, a density-dependent term and Coulomb potential for protons [25]. The parameters of the interaction are chosen as to reproduce basic nuclear matter properties and binding energies of finite nuclei. There are essentially two parametrizations of the Gogny force traditionally employed in nuclear structure calculations (D1S [28] and D1M [29]), whose parameters depend on the targets used in the fitting protocol. Recently, D1M*, a variant of D1M improving the symmetry energy properties, has been proposed [30]. Other recent proposals include the D2 force [31], with its finite range density dependent term, and the three-Gaussians variant D3G3 [32]. In the following, we will focus our attention in the more traditional D1S and D1M versions.

B. Orthogonality

As the ‘‘blocking’’ procedure is variational, it is often the case that two calculations starting with different multi-quasiparticle excitations having the same K and parity values end up in the same solution. Only in those cases where the starting MQP configurations differ in their deformation and pairing properties it is likely to find two differentiated solutions. The general solution to this problem is to introduce an orthogonality constraint in the self-consistent procedure. Fortunately, the number of possible configurations in high- K isomeric states is very limited (often just one) reducing the chances to find orthogonality issues in the calculations. The lower the K value of the excitation is the higher are the chances

to hit this problem. As discussed below, the situation is specially critical for $K = 0$ states. The study of low K excitations is a very interesting issue that deserves further consideration.

C. Equal filling approximation

The formalism presented above breaks time reversal invariance as the MQP excitation is not invariant under the action of the time reversal operator (converting the K quantum number into $-K$). This characteristic translates to the density matrix and pairing field entering the HFB equation and therefore time-odd contributions have to be considered in the Hartree-Fock (HF) and pairing fields. This is not a problem for the Gogny force, as the time-odd fields come directly from the interaction itself, but it can represent a problem for density functional such as some Skyrme variants or the Barcelona Catania Paris Madrid (BCPM) [33], which are not considering those contributions.

There is a formulation of the problem coined as the “equal filling approximation” (EFA) that preserves time reversal invariance and avoids time-odd fields characteristic of full blocking. This formulation was introduced heuristically many years ago to handle odd-mass nuclear systems and it was finally explained in terms of quantum statistical admixtures with specific probabilities in Ref. [34]. The EFA is known to provide similar results as the ones obtained in the full blocking formulation [35, 36] in the description of odd- A systems, demonstrating the minor role played by time-odd fields. The modification of the spectrum with respect to the perturbative one is mostly due to the quenching of pairing correlations in the two cases. The formulation of the EFA in terms of quantum statistical admixtures allows to generalize the EFA concept to the present case of MQP excitations. This generalization was discussed in detail in Ref. [36], and here we only recap the key concepts.

The density matrix for a multi-quasiparticle excitation is given by

$$\begin{aligned} \rho_{kk'}^{(\mu_{B_1}, \dots, \mu_{B_N})} &= \langle \Phi | \left(\prod_{\sigma=N}^1 \beta_{\sigma} \right) c_{k'}^{\dagger} c_k \left(\prod_{\sigma=1}^N \beta_{\sigma}^{\dagger} \right) | \Phi \rangle \\ &= (V^* V^T)_{kk'} + \sum_{\sigma} (U_{k'\sigma}^* U_{k\sigma} - V_{k'\sigma} V_{k\sigma}^*) , \end{aligned} \quad (19)$$

where $\sigma = \{\mu_{B_1}, \dots, \mu_{B_N}\}$ for a N -quasiparticle excitation. The EFA expression for the multi-quasiparticle excitation density is obtained from Eq. (19) by multiplying the sum on the right most term by one half and extending the sum on the label σ to include the time reverse quantum numbers of the set $\mu_{B_1}, \dots, \mu_{B_N}$. The same consideration applies straightforwardly to the EFA pairing tensor. Following the arguments of [36], it can be proved that the EFA density matrix and pairing tensors

can be obtained by introducing the statistical probabilities

$$p_{\sigma} = \begin{cases} 1 & \sigma \in \mu_{B_1}, \dots, \mu_{B_N}; \text{ or } \sigma \in \bar{\mu}_{B_1}, \dots, \bar{\mu}_{B_N} \\ 0 & \text{otherwise} \end{cases} . \quad (20)$$

D. Electromagnetic decay of high- K isomers

The electromagnetic decay of high- K isomers involves multitude of different configurations including many multi-quasiparticles excitations as well as different members of collective rotational bands. Given the very different intrinsic properties of the high- K isomers and the final states it is evident that the rotational formula commonly used to relate deformation parameters to transition probabilities [37] cannot be used here (see Ref [38] for an example of the failure of the rotational formula). Therefore, it is mandatory to carry out the calculation using wave functions in the laboratory frame, i.e. using the intrinsic states projected to good angular momentum [39]. This ambitious project is beyond the scope of the present work and will be addressed in the future.

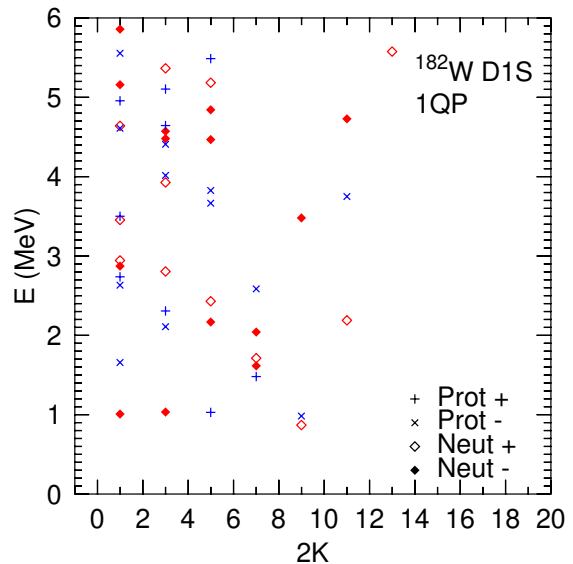


FIG. 3. One-quasiparticle excitation energies (in MeV) in ^{182}W for different values of the K quantum number. Positive (negative) parity proton excitations are represented by the + (x) symbol. For neutron excitations the symbols \diamond and \blacklozenge are used.

III. RESULTS AND DISCUSSIONS

There are many nuclei all over the nuclear chart with known high- K isomeric states [9]. It is not the purpose of this paper to discuss in detail the properties of all of them, but rather to show that the procedure discussed

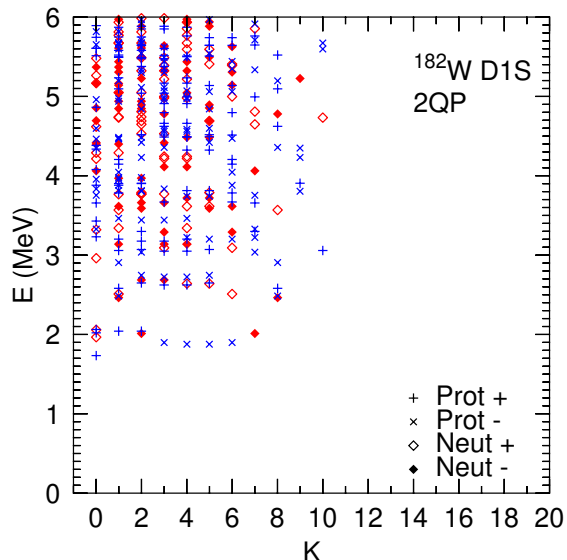


FIG. 4. Two-quasiparticles excitation energies (in MeV) in ^{182}W for different values of the combined K quantum number. Positive (negative) parity proton excitations are represented by the $+$ (\times) symbol. For neutron excitations the symbols \diamond and \blacklozenge are used.

above works in a set of selected examples and provides a reasonable account of excitation energies of the high- K states. One advantage in the calculation of high- K states compared to low- K states is that allows the neglect of orthogonality constraints. This is because it is very unlikely to find two or more low-lying states with the same (high) K values and similar mean-field properties (such as deformation parameters, pairing, etc.). Therefore, in the following we restrict our study to high- K isomeric states built on the ground state of even-even nuclei, and postpone the discussion of odd- A systems and fission isomers to a forthcoming publication.

A. The ^{254}No case

The heavy actinide ^{254}No is a typical example where two-quasiparticles excitations of both protons and neutrons lead to high- K isomeric states. In addition, four-quasiparticles excitations built on two-quasiparticles proton and neutron excitations lead to very high K values for the associated states [3, 6, 26]. There are several known isomeric states in this nucleus being the $K = 16^+$ four-quasiparticles excitation the best known example. This four-quasiparticles excitation with a half-life of $184 \mu\text{s}$ is made of a two-quasiparticles excitation of protons in $\Omega = 9/2$ and $\Omega = 7/2$ orbitals together with a two-neutrons excitation from the same orbitals. In addition to this isomer there are others, like the $K = 3^+$ (two-quasiparticles proton excitation) and two $K = 8^-$ states (one corresponding to a two-protons excitation, and the other to a two-neutrons excitations). The $K = 3^+$ state is ob-

tained from the excitation of protons in orbitals $\Omega = 7/2$ and $\Omega = -1/2$ close to the Fermi level and is the signature partner of a $K = 4^+$ state not found experimentally yet. For a detailed discussion of relevant single particle orbitals in this nucleus obtained with different interactions the reader is referred to Ref [40]. Additional two-neutrons quasiparticle states like the $K = 10^+$ are observed [27]. The experimental spectrum along with the results obtained with the Gogny D1S and D1M parametrizations are shown in Fig. 1. A careful analysis of the properties of the MQP excitations leads to the conclusion that pairing correlations are severely quenched in the isospin channel of the excitation. As a consequence, the four quasiparticle $K = 16^+$ state shows almost no static pairing correlations. This general feature of MQP excitations call for a more developed and consistent treatment of dynamic pairing correlations [41], by considering the effect of particle-number restoration before variation and fluctuations on the pairing-gap order parameter.

From these results, we can conclude that the impact of using D1S or D1M parametrization of the Gogny force is small for excitation energies, resulting in the same level of confidence in studying high- K isomeric states.

It is also interesting to explore the results obtained with the EFA, discussed above. In Fig. 1 the results obtained with Gogny D1S employing both the blocking and EFA approximation are compared with the experimental data. The results of the EFA are qualitatively similar to the ones from full blocking indicating the little impact of time-odd fields in the excitation energies of the high K states. As in the full blocking case discussed above, pairing correlations are severely quenched in the EFA. Additionally, one observes that the deformation parameters of both the blocking and EFA results are very close to each other. The good match between the full blocking and EFA results can represent a simplification in the theoretical calculations as the time-reversal preserving character of EFA simplifies the calculations. However, it has to be kept in mind that the EFA does not provide a wave function and therefore the calculation of transition probabilities requires further assumptions not present in the full-blocking case.

Finally, we conclude that the comparison between experimental data and theoretical calculations is satisfactory, particularly taking into account that the Gogny forces were not fitted specifically to reproduced single particle properties in the region of interest.

B. The ^{178}Hf case

The high- K isomers of the rare-earth nucleus ^{178}Hf are also prototypical examples of high- K states, mostly because the 16^+ one has a lifetime of 31-yr, the longest among all the know high- K isomeric states in even-even nuclei. Again, we observe several two-quasiparticles excitations of proton and neutron character as well as four-quasiparticles (two-protons and two-neutron) states. The

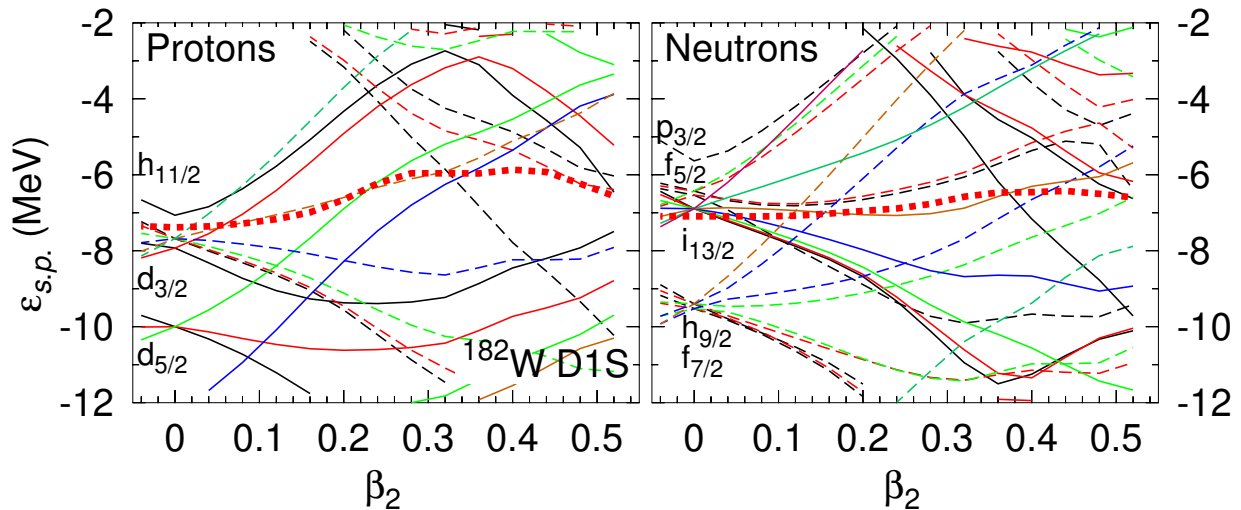


FIG. 5. Single particle energies (in MeV) for protons and neutrons in the isotope ^{182}W are drawn as a function of the β_2 deformation parameters. Full (dashed) lines correspond to positive (negative) orbitals. The color code corresponds to the value of the Ω quantum number of the single particle orbital: black, $\Omega = 1/2$; red, $\Omega = 3/2$; green, $\Omega = 5/2$; blue, $\Omega = 7/2$; etc. The Ω quantum number of each orbital can also be inferred from the behavior of the single particle energies near sphericity. The thick dotted line corresponds to the Fermi level

lowest energy 8^- states is a two-neutrons excitation with particles being promoted to the $\Omega = 9/2^+$ orbital (from the $i_{13/2}$), and the $\Omega = 7/2^-$ orbital (from the spherical $h_{9/2}$). On the other hand, the next 8^- states is a two-protons excitation with particles being promoted to the $\Omega = 9/2^-$ orbital (from the $h_{11/2}$) and the $\Omega = 7/2^+$ orbital (from the $g_{7/2}$ spherical orbital). The combined excitation of the two-protons and two neutrons make the $K = 16^+$ isomer. The assignments of the two 8^- states and the 16^+ agree with the calculations of Ref. [17] using the projected shell model (PSM). Finally, the 6^+ state is a two-protons excitation involving the $\Omega = 5/2^+$ orbital (from the $d_{5/2}$) and the $\Omega = 7/2^+$ orbital (from the $g_{7/2}$ spherical orbital). The combined excitation of this proton 6^+ excitation and the 8^- one discussed above is responsible for the 14^- state. The assignment of the 6^+ state differs from the one of [17], where it is claimed to be a two-neutrons excitation instead. The origin of the discrepancy between Ref. [17] and this work could be related to the many-body method used in the PSM calculations of [17], which introduces correlations beyond mean-field not present in our approach. However, the PSM interaction employed in [17] is schematic and restricted to have a fixed value of quadrupole deformation parameters and pairing strengths for all the quasiparticle configurations. This limitation compares with the richness of the Gogny force in describing nuclear phenomena all over the nuclide chart [25]. The assignment of deformed single particle orbitals to spherical orbits discussed in previous paragraphs can be obtained from Fig. 5, where the single particle spectrum as a function of quadrupole deformation parameter β_2 and for the nearby ^{182}W isotope is displayed. Regarding the comparison of our results with experimen-

tal data in both D1S and D1M cases one can conclude that it is outstanding, giving credit to the claimed universality of the Gogny interaction. Both parametrizations are able to reproduce the physics of high- K isomers with the same set of parameters not only in the superheavies (^{254}No), but also in the rare-earth region. As in the nobelium case, pairing correlations are strongly suppressed and the quenching is responsible for the reordering of the spectrum as compared to the perturbative results obtained without selfconsistency. As mentioned before, the strong suppression of pairing suggests an appropriate treatment of dynamic pairing correlations.

As in the previous example, we have carried out calculations with Gogny D1S using the EFA. The results are compared with the ones obtained with full blocking and the experimental data in Fig. 2. As in the nobelium case, the results are very similar to those obtained with full blocking, indicating the minor role played by time-odd fields in the excitation energy of the isomers.

C. The tungsten isotopic chain

The region around $Z = 72$ (Hf) and $N = 106$ is known to have all the required characteristics to show low lying high- K isomeric states [7], namely the existence of high- K single particle orbits around the Fermi level. One of the species in the region with a large number of known isomers is tungsten ($Z = 74$) and therefore its isotopes represent good candidates for high- K isomer studies [42]. As in previous examples, we restrict to even-even nuclei only and postpone the study of odd- A isotopes to a forthcoming study. Additionally, tungsten isotopes have been

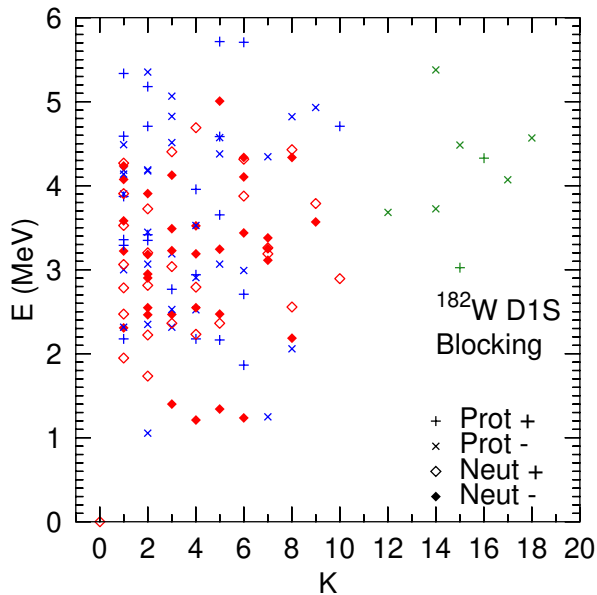


FIG. 6. Self-consistent two-quasiparticles excitation energies (in MeV) for the ^{182}W isotope. The assignment of each symbol (and color) is the same as in Fig. 4. Four-quasiparticles excitations composed of 2qp proton and 2qp excitations are also shown with green crosses (plus) symbols for negative (positive) parity states. The latter can be easily identified, as they are the only excitations with $K > 10$.

thoroughly studied with the PSM approach [19, 43].

In Fig. 3 we show, for the nucleus ^{182}W , the lowest one-quasiparticle (1qp) excitation energies for both protons and neutrons labelled with both the K and parity quantum numbers (no octupole correlations are present in this case). Five quasiparticles are located at around 1 MeV excitation energy, and two of them have specially large K values: a $K^\pi = 9/2^+$ neutron and a $K^\pi = 9/2^-$ proton excitation. At slightly higher energies one observes three $K = 7/2$ states, one for protons, two for neutrons. When combined together with the $K = 9/2$ one-quasiparticle states they form high- K low lying 2qp excitations. The complete perturbative spectrum of two-quasiparticle states is shown in Fig. 4. The perturbative spectrum is obtained by considering both positive and negative (i.e., the time reserved of the positive) K values for each 1qp state in order to obtain degenerated signature partners. In this plot, one observes the characteristic ~ 2 MeV gap in excitation energy, which is the consequence of the rather strong pairing correlations both for protons (pairing gap $\Delta_p = 0.71$ MeV) and neutrons ($\Delta_n = 0.80$ MeV). Also, in the range of excitation energies below 6 MeV included in the plot, there are no 2qp excitations with K larger than 10, indicating that higher K excitations in the region must necessarily have a 4qp character. Many 2qp excitations are observed in the considered energy window, the number of them with a given K value decreases with increasing K , being maximal for $K = 0$ excitations.

In order to understand the characteristics of some of the discussed quasiparticle states it is convenient to look at the single particle energies, plotted as a function of the deformation parameter β_2 in Fig. 5. In separate panels the corresponding plots for both protons and neutrons are shown. Full (dashed) lines correspond to positive (negative) parity levels. The Ω values for each individual single particle state follow a color code (black for $\Omega = 1/2$, red for $\Omega = 3/2$, green for $\Omega = 5/2$, etc.), but their values can also be inferred by looking at the splitting of spherical single particle levels when the quadrupole prolate deformation is switched on. At the typical deformation of the ground state of the tungsten isotopes considered, $\beta_2 \approx 0.25$, there is a positive parity state close to the Fermi level (the thick dashed line) with $\Omega^\pi = 5/2^+$ (coming from the $d_{5/2}$ and with asymptotic Nilsson quantum numbers [402]5/2), and a negative parity one with $\Omega^\pi = 9/2^-$ (coming from the $h_{11/2}$ and with asymptotic Nilsson quantum numbers [514]9/2). In the neutron side, there is a $\Omega^\pi = 9/2^+$ close to the Fermi level and coming from the $i_{13/2}$ orbital ([624]9/2), and two negative parity orbitals coming from the $f_{5/2}$ spherical orbital and Ω^π values of $1/2^-$ ([510]1/2) and $3/2^-$ ([512]3/2). These single particle levels are responsible for the five 1qp excitations with energies around 1 MeV discussed in Fig. 3.

Selected 2qp and 4qp excitations obtained after self-consistent full blocking are shown in Fig. 6 for the nucleus ^{182}W . As the orthogonality constraint has not been imposed in the calculations many 2qp perturbative excitations converge, after the self-consistent procedure, to the lowest excited state with the same K and parity values. This is the reason why one observes much less states than the ones shown in Fig. 3. This is particularly important for $K = 0$ states, where only the ground state is obtained in the calculation if no orthogonality constraint is imposed. As the coexistence of multiple $K = 0^+$ states is an interesting field of research by itself [50], it will be the subject of a future study exploring the impact of the orthogonality constraint in MQP excitations. In the plot we show, along with the 2qp excitations, selected 4qp excitations with K values larger than 10. In all the cases, the 4qp excitations correspond to a 2qp proton and a 2qp neutron multi-quasiparticle excitation. The lowest 2qp excitation energies are slightly above 1 MeV, as compared to the perturbative 2qp excitation energies that are around 2 MeV. This reduction of almost one MeV indicates the importance of self-consistency in the determination of the excitation energies of the multi-quasiparticle states. The origin of the excitation energy reduction can be traced back to the severe quenching of pairing correlation in the isospin channel of the excitation. As the ground state pairing gap for both types of nucleon is roughly 0.7 MeV for protons and 0.8 MeV for neutrons, its disappearance explains the almost 1 MeV reduction obtained in the blocking procedure.

Given that, in spite of the limitations imposed by not considering the orthogonality constraint, the number of 2qp excitations is huge, a comparison with experimen-

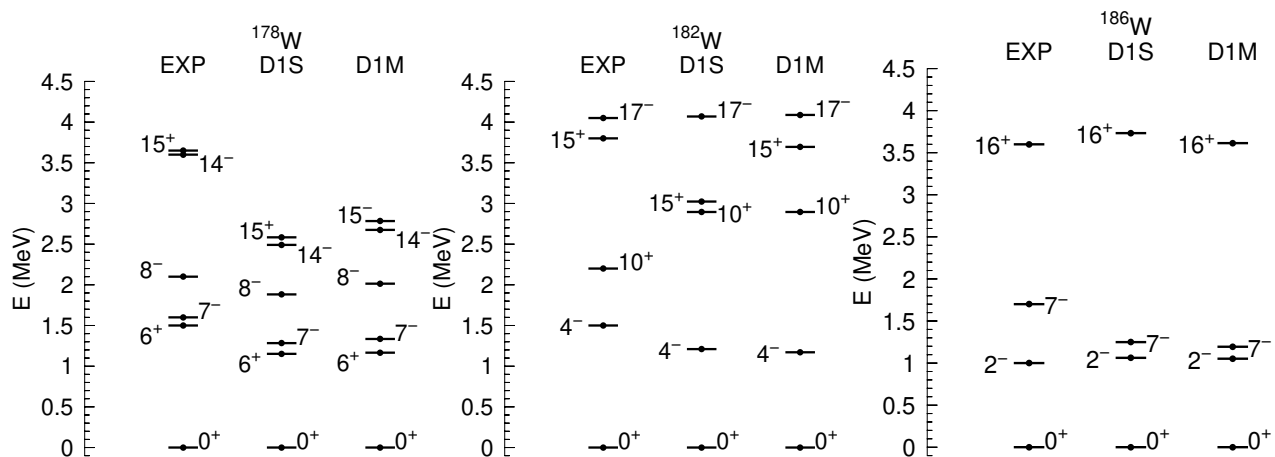


FIG. 7. Comparison of theoretical results obtained with Gogny D1S and D1M, and experimental data [4, 9, 44–49] (and references therein), for relevant high- K excitations known experimentally in ^{178}W , ^{182}W , and ^{186}W .

tal data is meaningless except for singular states, like the high- K isomers under analysis. The singularity of those states resides in their large K values, the very limited number of them and their long lifetimes. In order to compare with experimental data it is therefore necessary to proceed as in the previous cases and limit the comparison to those states that have been measured. In the theoretical side, one considers the lowest energy state with the same K quantum number as the experimental one. Such a comparison is made in Fig. 7 where the results of the calculations for ^{178}W , ^{182}W , and ^{186}W are shown.

In ^{178}W , the 6^+ is a two-neutrons excitation of orbitals with $\Omega = 7/2$ and $\Omega = 5/2$. The 7^- is also a two-neutrons excitation with two $\Omega = 7/2$ orbitals of opposite parity involved. On the other hand, the 8^- is a two-proton state made of a $\Omega = 7/2$ orbital and a $\Omega = 9/2$ one. The 14^- and 15^+ are four-quasiparticles excitations made of the two-protons excitation with $K = 8^-$ and the 6^+ and 7^- two-neutrons excitations, respectively. Our results agree with the experimental data of Purry *et al* [46] and the mic-mac model results of Xu *et al* [15]. In this nucleus there are many more high- K isomeric states known experimentally, including eight quasiparticle excitations made of four-proton and four-neutron quasiparticle excitations [46]. They will be the subject of a more detailed study in the future. In ^{182}W , both the 4^- and the 10^+ are two-neutrons excitations, the first involving $\Omega = 9/2$ and $\Omega = -1/2$ single particle orbitals and the other $\Omega = 9/2$ and $\Omega = 11/2$ ones. On the other hand, the 15^+ and 17^- states are four-quasiparticles excitations, two-neutrons and two-protons. The two-protons excitation involves $\Omega = 9/2$ and $\Omega = 5/2$ orbitals providing $K = 7$ and negative parity. The 17^- is the combination of the $K = 7^-$ two-protons excitation and the two-neutrons $K = 10^+$ excitation, whereas the 15^+ requires a $K = 8^-$ two-neutrons excitation. Additionally, in ^{186}W , the $K = 7^-$ is the two-protons excitation observed in ^{182}W . The 2^- is the part-

ner of the $K = 7^-$ with one of the orbitals reversed in time. Finally, the 16^+ is made of the two-protons excitation with $K = 7^-$ and a two-neutrons excitation with $K = 9^-$, consequence of the excitation of neutron single particle orbitals with $\Omega = 7/2$ and $\Omega = 11/2$.

The comparison with experimental data for the set of tungsten isotopes considered is very good, taking into account the global character of the family of Gogny forces considered in this paper. The limited number of parameters (14) is universal for all nuclei in the nuclear chart and all kind of phenomena. It is obvious then that such a global interaction cannot provide spectroscopic accuracy for the excitation energies of non-collective states at the level of other many-body methods and/or interactions. Spectroscopic quality can only be attained if specifically tailored-to-the-region interactions with tens or even hundred of parameters are used. One has also to take into account that the mean-field method being used in the present calculation is not including beyond mean-field correlations like those stemming from symmetry restoration and/or particle-vibration coupling. Those correlations can amount to energy differences between states of hundreds of keV and, if they are not explicitly considered, it is not possible to extract a final conclusion regarding the quality of the interaction with respect to experimental data. Taking these considerations into account, one could consider satisfactory to obtain excitations energies differing by hundred keV (or even one MeV) from experiment. This is because, in spite of these discrepancies, the predictions made by the present calculations can be a good guidance to experimental proposals and can also help to identify the origin of such excitations (deformation, pairing properties, etc.).

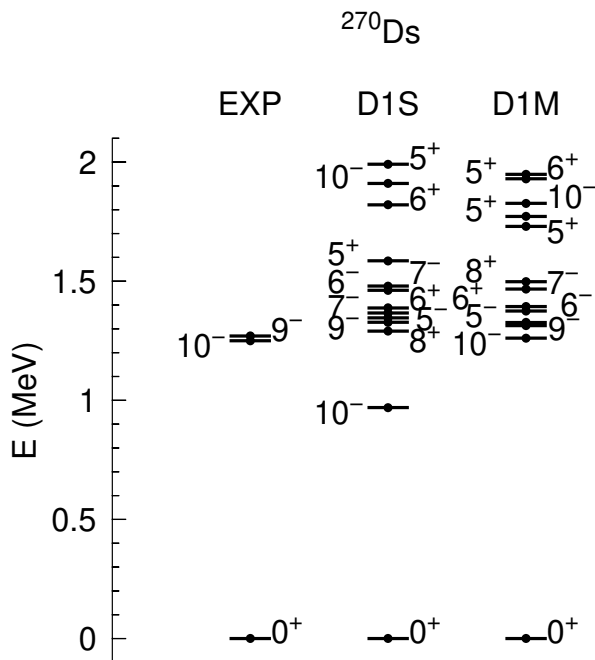


FIG. 8. Comparison of high- K isomeric states in ^{270}Ds predicted by Gogny D1S and D1M, and experimental data [6, 51].

D. Superheavy nuclei: the ^{270}Ds case

In Hofmann *et al.* [51] the synthesis of the isotope of darmstadtium with $A = 270$ and the identification of its decay products were reported. Along with the ground state, the decay of a high- K isomer with a half-life in the millisecond range was identified. With this discovery, ^{270}Ds is the heaviest nucleus where a high- K isomeric state has been found [6]. The excitation energy of the isomer was estimated to be 1.13 MeV, in good agreement with results of HFB calculations reported in the same reference. The results of our calculation with both D1S and D1M parametrizations of Gogny are shown in Fig. 8, along with experimental data. The experimental excitation energy of both the 9^- and 10^- states [6] is well reproduced in the two cases and those states are assigned to a two-neutrons excitation. Along with the known experimental isomers, a bunch of other two-quasiparticles isomeric states with K greater than 5 are predicted by the calculations and shown in the plot with the purpose to demonstrate that there are many more predicted isomeric states than the ones measured experimentally. For instance, the lowest 5^- , 6^- and 7^- are two-neutrons excitations involving a $\Omega = 11/2$ orbital. On the other hand, the lowest 6^+ is a two-protons excitation. The predicted states indicate that ^{270}Ds is a good candidate for experimental search of isomeric states. In the calculation, the quadrupole β_2 deformation parameter of the ground

state and all isomeric states is essentially the same (up to one or two percent), with a value $\beta_2 = 0.245$. Reflection asymmetry is not present in the states displayed.

IV. CONCLUSIONS AND OUTLOOK

In this paper we present blocking calculations of two- and four-quasiparticle excitations leading to high- K isomeric states in several relevant examples across the nuclear chart. The blocking procedure is presented in detail by using a novel approach involving “swap” matrices. For the interaction, the Gogny force with the D1S and D1M parametrizations is used. The density prescription concerning density-dependent interactions is discussed, and it is shown that the “rearrangement effects” in the definition of quasiparticle energies shall be taken into account. As typical cases in different regions of the nuclear chart we have carried out calculations in the superheavy ^{254}No , the rare-earth ^{178}Hf , several tungsten isotopes and the super-heavy ^{270}Ds . The agreement with experimental data is very good, particularly in the light of the parameter-free character of these calculations. The Gogny interaction is a global EDF adjusted to bulk nuclear properties, designed to provide a reasonable description of all kind of nuclear properties all over the nuclear chart. Additional calculations with the equal filling approximation show an almost perfect matching with the blocking ones. This result indicates that the effect of time-odd fields in multi-quasiparticle excitations is minor, and most of the reduction in the excitation energy (as compared to the sum of one-quasiparticle excitations) arises from the quenching of pairing correlations. Finally, a detailed study and comparison with experimental data is carried out in a series of tungsten isotopes. The good agreement with experimental data obtained for excitation energies give us confidence that effective forces like Gogny can be confidently used to describe high- K excitations all over the nuclear chart. The results open the door to the inclusion of sophisticated beyond mean-field effects such as symmetry restoration, that will allow for a better and more systematic treatment of the electromagnetic decay out of such high- K isomeric states. The formalism also allows for the inclusion of fluctuation in collective degrees of freedom opening the possibility to study particle-vibration coupling from a microscopic perspective. The possibility to easily implement an orthogonality constraint also opens the door to a systematic study of 0^+ excited states in even-even nuclei.

ACKNOWLEDGMENTS

The author thanks S. Giuliani for useful discussions. This work has been supported by the Spanish Agencia Estatal de Investigación (AEI) of the Ministry of Science and Innovation (MCIN) under grant agreement No. PID2021-127890NB-I00.

- [1] P. Walker and G. Dracoulis, *Nature* **399**, 35 (1999).
- [2] P. M. Walker and G. D. Dracoulis, *Hyperfine Interactions* **135**, 83 (2001).
- [3] R.-D. Herzberg, P. T. Greenlees, P. A. Butler, G. D. Jones, M. Venhart, I. G. Darby, S. Eeckhaudt, K. Eskola, T. Grahm, C. Gray-Jones, F. P. Hessberger, P. Jones, R. Julin, S. Juutinen, S. Ketelhut, W. Korten, M. Leino, A.-P. Leppanen, S. Moon, M. Nyman, R. D. Page, J. Pakarinen, A. Pritchard, P. Rahkila, J. Saren, C. Scholey, A. Steer, Y. Sun, C. Theisen, and J. Uusitalo, *Nature* **442**, 896 (2006).
- [4] F. Kondev, G. Dracoulis, and T. Kibédi, *Atomic Data and Nuclear Data Tables* **103-104**, 50 (2015).
- [5] G. D. Dracoulis, P. M. Walker, and F. G. Kondev, *Reports on Progress in Physics* **79**, 076301 (2016).
- [6] D. Ackermann and C. Theisen, *Physica Scripta* **92**, 083002 (2017).
- [7] P. Walker and Z. Podolyák, *Physica Scripta* **95**, 044004 (2020).
- [8] A. Aprahamian and Y. Sun, *Nature Physics* **1**, 81 (2005).
- [9] S. Garg, B. Maheshwari, B. Singh, Y. Sun, A. Goel, and A. K. Jain, *Atomic Data and Nuclear Data Tables* **150**, 101546 (2023).
- [10] G. W. Misch, T. M. Sprouse, and M. R. Mumpower, *The Astrophysical Journal Letters* **913**, L2 (2021).
- [11] S.-i. Fujimoto and M.-a. Hashimoto, *Mon. Not. R. Astron. Soc. Lett.* **493**, L103 (2020), arXiv:2001.10668.
- [12] G. W. Misch, T. M. Sprouse, M. R. Mumpower, A. J. Couture, C. L. Fryer, B. S. Meyer, and Y. Sun, *Symmetry* **13**, 10.3390/sym13101831 (2021).
- [13] W. Nazarewicz, M. Riley, and J. Garrett, *Nuclear Physics A* **512**, 61 (1990).
- [14] P. Jachimowicz, M. Kowal, and J. Skalski, *Phys. Rev. C* **92**, 044306 (2015).
- [15] F. Xu, P. Walker, J. Sheikh, and R. Wyss, *Physics Letters B* **435**, 257 (1998).
- [16] K. Hara and Y. Sun, *International Journal of Modern Physics E* **04**, 637 (1995).
- [17] Y. Sun, X.-R. Zhou, G.-L. Long, E.-G. Zhao, and P. M. Walker, *Physics Letters B* **589**, 83 (2004).
- [18] P. Ring and P. Schuck, *The nuclear many body problem* (Springer, Berlin, 1980).
- [19] X.-Y. Wu, S. K. Ghorui, L.-J. Wang, Y. Sun, M. Guidry, and P. M. Walker, *Phys. Rev. C* **95**, 064314 (2017).
- [20] G. F. Bertsch and L. M. Robledo, *Phys. Rev. Lett.* **108**, 042505 (2012).
- [21] L. M. Robledo, *Phys. Rev. C* **79**, 021302 (2009).
- [22] J.-P. Delaroche, M. Girod, H. Goutte, and J. Libert, *Nuclear Physics A* **771**, 103 (2006).
- [23] J.-P. Blaizot and G. Ripka, *Quantum theory of finite systems* (The MIT press, 1986).
- [24] H. Kasuya and K. Yoshida, *Progress of Theoretical and Experimental Physics* **2021**, 013D01 (2020), <https://academic.oup.com/ptep/article-pdf/2021/1/013D01/36123331/ptaa163.pdf>.
- [25] L. M. Robledo, T. R. Rodríguez, and R. R. Rodríguez-Guzmán, *Journal of Physics G: Nuclear and Particle Physics* **46**, 013001 (2019).
- [26] S. K. Tandel, P. Chowdhury, E. H. Seabury, I. Ahmad, M. P. Carpenter, S. M. Fischer, R. V. F. Janssens, T. L. Khoo, T. Lauritsen, C. J. Lister, D. Seweryniak, and Y. R. Shimizu, *Phys. Rev. C* **73**, 044306 (2006).
- [27] R. Clark, K. Gregorich, J. Berryman, M. Ali, J. Allmond, C. Beausang, M. Cromaz, M. Deleplanque, I. Dragojević, J. Dvorak, P. Ellison, P. Fallon, M. Garcia, J. Gates, S. Gros, H. Jeppesen, D. Kaji, I. Lee, A. Macchiavelli, K. Morimoto, H. Nitsche, S. Paschalis, M. Petri, L. Stavsetra, F. Stephens, H. Watanabe, and M. Wiedeking, *Physics Letters B* **690**, 19 (2010).
- [28] J. F. Berger, M. Girod, and D. Gogny, *Nucl. Phys. A* **428**, 23 (1984).
- [29] S. Goriely, S. Hilaire, M. Girod, and S. Péru, *Phys. Rev. Lett.* **102**, 242501 (2009).
- [30] C. Gonzalez-Boquera, M. Centelles, X. Viñas, and L. Robledo, *Physics Letters B* **779**, 195 (2018).
- [31] F. Chappert, N. Pillet, M. Girod, and J.-F. Berger, *Phys. Rev. C* **91**, 034312 (2015).
- [32] L. Batail, D. Davesne, S. Péru, P. Becker, A. Pastore, and J. Navarro, *The European Physical Journal A* **59**, 173 (2023).
- [33] M. Baldo, L. M. Robledo, and X. Viñas, *Eur. Phys. J. A* **59**, 156 (2023).
- [34] S. Perez-Martin and L. M. Robledo, *Phys. Rev. C* **78**, 014304 (2008).
- [35] N. Schunck, J. Dobaczewski, J. McDonnell, J. Moré, W. Nazarewicz, J. Sarich, and M. V. Stoitsov, *Phys. Rev. C* **81**, 024316 (2010).
- [36] S. Giuliani and L. Robledo, Submitted to *Physical Review C* (2023).
- [37] A. Bohr and B. Mottelson, *Nuclear Structure*, Vol. II (Benjamin, New-York, 1975).
- [38] L. M. Robledo and G. F. Bertsch, *Phys. Rev. C* **86**, 054306 (2012).
- [39] J. A. Sheikh, J. Dobaczewski, P. Ring, L. M. Robledo, and C. Yannouleas, *Journal of Physics G: Nuclear and Particle Physics* **48**, 123001 (2021).
- [40] J. Dobaczewski, A. Afanasjev, M. Bender, L. Robledo, and Y. Shi, *Nuclear Physics A* **944**, 388 (2015), special Issue on Superheavy Elements.
- [41] D. Almeded, S. Frauendorf, and F. Dönau, *Phys. Rev. C* **63**, 044311 (2001).
- [42] D. M. Cullen, S. L. King, A. T. Reed, J. A. Sampson, P. M. Walker, C. Wheldon, F. Xu, G. D. Dracoulis, I.-Y. Lee, A. O. Macchiavelli, R. W. MacLeod, A. N. Wilson, and C. Barton, *Phys. Rev. C* **60**, 064301 (1999).
- [43] C. Jiao, Y. Shi, F. Xu, Y. Sun, and P. M. Walker, *Science China Physics, Mechanics and Astronomy* **55**, 1613 (2012).
- [44] P. Regan, P. Walker, G. Dracoulis, S. Anderssen, A. Byrne, P. Davidson, T. Kibédi, G. Lane, A. Stuchbery, and K. Yeung, *Nuclear Physics A* **567**, 414 (1994).
- [45] T. Shizuma, S. Mitarai, G. Sletten, R. Bark, N. Gjørup, H. Jensen, J. Wrzesinski, and M. Piiparinen, *Nuclear Physics A* **593**, 247 (1995).
- [46] C. Purry, P. Walker, G. Dracoulis, T. Kibédi, F. Kondev, S. Bayer, A. Bruce, A. Byrne, W. Gellertly, P. Regan, C. Thwaites, O. Burglin, and N. Rowley, *Nuclear Physics A* **632**, 229 (1998).
- [47] C. M. Baglin, *Nuclear Data Sheets* **99**, 1 (2003).
- [48] E. Achterberg, O. Capurro, and G. Marti, *Nuclear Data Sheets* **110**, 1473 (2009).

- [49] B. Singh and J. C. Roediger, [Nuclear Data Sheets](#) **111**, 2081 (2010).
- [50] D. Meyer, V. Wood, R. Casten, C. Fitzpatrick, G. Graw, D. Bucurescu, J. Jolie, P. von Brentano, R. Hertenberg, H.-F. Wirth, N. Braun, T. Faestermann, S. Heinze, J. Jerke, R. Krücken, M. Mahgoub, O. Möller, D. Mücher, and C. Scholl, [Physics Letters B](#) **638**, 44 (2006).
- [51] S. Hofmann, F. P. Heßberger, D. Ackermann, S. Antalic, P. Cagarda, S. Ćwiok, B. Kindler, J. Kojouharova, B. Lommel, R. Mann, G. Münzenberg, A. G. Popeko, S. Saro, H. J. Schött, and A. V. Yeremin, [The European Physical Journal A - Hadrons and Nuclei](#) **10**, 5 (2001).